

**Kinetics of Flux Jumps in Type-II Superconductors\***

R. B. Harrison and L. S. Wright

*Royal Military College of Canada, Kingston, Ontario, Canada*

M. R. Wertheimer

*Canadian Liquid Air, Montreal, Quebec, Canada*

(Received 17 July 1972)

Magneto-optic techniques coupled with high-speed cinematography have been used to study the kinetics of flux jumps in type-II superconducting disk samples. The time dependence of the distance of advance (penetration) of the flux front from the point of origin of the jump is shown to be well described by an equation of the form  $Z = Z_{\infty}(1 - e^{-t/\tau})$ . This correspondence strongly suggests that flux motion during a "runaway instability," at least under these experimental conditions, can be more accurately explained in terms of viscous damping than by a diffusion law. If the flux-jump volume is simulated by a short cylindrical conductor, a time constant can be calculated for the  $LR$  circuit analog. The time constants calculated from this rather crude model compare favorably with experimentally measured values of  $\tau$  for a large range of sample materials and geometries.

Although several theoretical treatments of flux jumping have been published in recent years,<sup>1-3</sup> these have dealt primarily with a formulation of the conditions giving rise to a flux jump or "runaway instability." The problem of describing what happens when the moving flux has reached runaway speed is a formidable one involving many variables. The present paper reports experimental data on this latter aspect of flux jumping.

By using the Faraday rotation technique in conjunction with high-speed cinematography, it has been possible to study the kinetics of flux jumps in disk-shaped bulk samples.<sup>4-6</sup> Figure 1 shows the position of the boundary between the superconducting and mixed states taken from successive frames of a cinefilm recorded at a speed of 10 200 frames/sec in a cold-rolled Nb-25-at. %-Zr disk (sample

NZP5; diameter  $d = 18.0$  mm, thickness  $h = 2.0$  mm). A similar contour diagram for a pure niobium sample (No. 77) was shown in Ref. 4. In the present experiments the sample was immersed in He II at 1.4 K, and an axial field from a superconducting solenoid was swept up from an original value of zero at a rate of 122 Oe/sec. The first flux jump, which occurred at a field of  $H_{fj} = 1980 \pm 30$  Oe, was recorded on Ektachrome 7242 color film using a Redlake HYCAM rotating-prism camera.

In Fig. 2,  $Z$ , the distance between the flux front and the point of origin of the jump, is shown plotted against time  $t$ . Also plotted are data pertaining to niobium, sample 77. The solid curves represent best fits of the form

$$Z = Z_{\infty}(1 - e^{-t/\tau}), \tag{1}$$

where  $Z_{\infty}$  is the terminal penetration distance of the completed jump and  $\tau$  is the time constant. These quantities, as well as the mean width  $w$  of

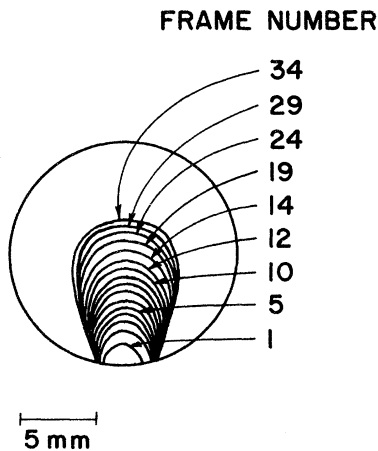


FIG. 1. Successive positions of the flux front for the first flux jump in Nb-25-at. %-Zr specimen NZP5. The time interval between frames is 98  $\mu$ sec. The numbers refer to the frames from which the contours were traced.

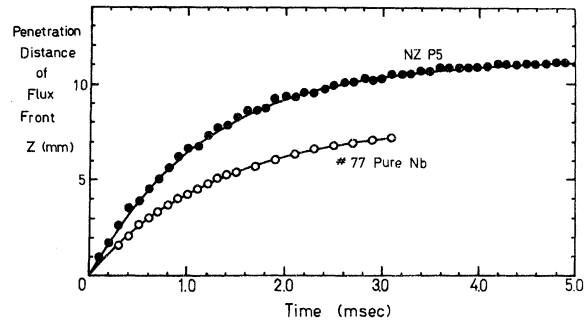


FIG. 2. Position of the flux front relative to the origin of the jump as a function of time. Curves 1 and 2 show experimental data and empirical best-fit curves for samples NZP5 and Nb specimen 77, respectively.

the flux-penetrated region, are highly reproducible under constant experimental conditions, as is shown in Table I.

During a runaway instability, the forces acting on a moving flux element are  $F_L = F_P + F_V$ ; they are, respectively, the Lorentz force, the pinning force, and a viscous drag force which is proportional to the velocity of the flux line. The viscosity is related to the flux-flow resistivity  $\rho_f$ , which is, in turn, related to the normal resistivity of the material<sup>7</sup>:

$$\rho_f = \rho_n B / H_{c2}(0), \quad (2)$$

where  $B$  is the magnetic induction inside the specimen and  $\rho_n$  is the normal-state resistivity of the specimen material. The correspondence shown in Fig. 2 between Eq. (1) and the experimental data suggests strongly that the kinetics of flux motion during a flux jump are controlled by viscous damping.

In earlier work,<sup>4,5</sup> the data were analyzed in terms of a diffusion law; plots of  $Z^2$  vs  $t$  were usually linear for  $0 < Z < 0.8 Z_\infty$  but not for  $Z > 0.8 Z_\infty$ . In the case of sample 77, the flux penetrated about 40% of the sample's diamagnetic portion and the deviation from linearity was explained qualitatively in terms of a change in the demagnetizing coefficient  $n$ . The smaller jumps in sample NZP5, which occupy only about 25% of the original diamagnetic volume, prompted us to reexamine this viewpoint: A rough calculation revealed that  $n$  only changed by a few percent during a flux jump.

The form of the curves in Fig. 2 suggests a simple  $LR$  circuit analog. If we simulate the flux-penetrated region of the jump by a short cylindrical conductor, the inductance (in  $\mu\text{H}$ ) is given by<sup>8</sup>

$$L = 2 \times 10^{-3} Z_\infty [\ln(2Z_\infty/r) + r/Z_\infty - 0.75], \quad (3)$$

where  $r = (wh/\pi)^{1/2}$ ,  $h$  is the sample thickness,  $w$  is the average width of the jump zone, and  $Z_\infty$  is the terminal penetration distance of the jump. Possible contributions from the shielding-current region around the sample perimeter have been calculated and found to be negligible.

Wertheimer and Gilchrist<sup>5</sup> have found that the resistivity "seen" by eddy currents in the wake of the runaway flux front is  $\rho_f$ . Consequently, the resistance of the inductor analog is given by

TABLE I. Terminal penetration distance  $Z_\infty$ , mean width of the flux-penetrated region  $w$ , and time constant  $\tau$ .

Sample	$Z_\infty$ (cm)	$w$ (cm)	$\tau$ (msec)
NZP 5	$1.06 \pm 0.08$	$0.65 \pm 0.07$	$1.16 \pm 0.03$
Nb 77	$0.79 \pm 0.05$	$0.75 \pm 0.07$	$1.33 \pm 0.05$

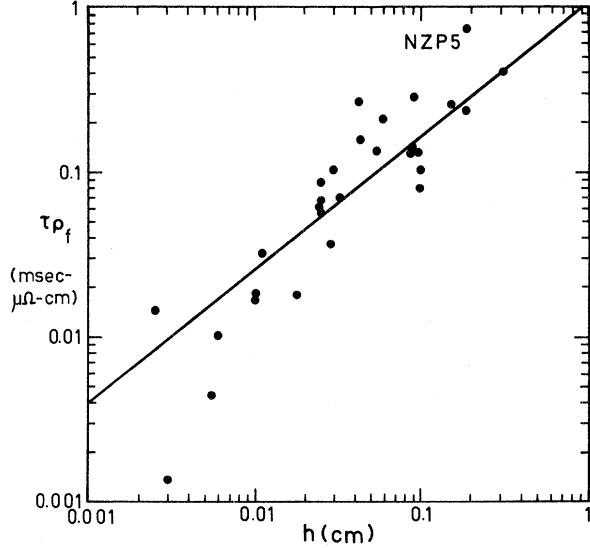


FIG. 3. Plot of experimental values of  $\tau\rho_f$  (msec  $\mu\Omega$  cm) vs specimen thickness  $h$ . The straight line represents Eq. (5) and the data points correspond to the specimens used in Ref. 5 and the present experiments.

$$R = \frac{\rho_f}{\pi} \frac{Z_\infty}{r^2} = \frac{\rho_f Z_\infty}{wh} \quad (4)$$

and the time constant  $\tau$  of the  $LR$  circuit is

$$\tau = \frac{L}{R} = 2 \times 10^{-3} \frac{wh}{\rho_f} \left( \ln \frac{2Z_\infty}{(wh/\pi)^{1/2}} + \frac{(wh/\pi)^{1/2}}{Z_\infty} - 0.75 \right), \quad (5)$$

where  $\tau$  is in seconds and  $\rho_f$  is in  $\mu\Omega$  cm.

In Fig. 3,  $\tau\rho_f$  is plotted against sample thickness  $h$  for the experimental data of Ref. 5 and the present experiments. (In most cases  $\tau$  represents the average duration of the jump rather than a specific exponential time constant.) The flux jumps measured and analyzed in Ref. 5 were quite similar in size and shape, so that average values of the final width ( $w=0.5$  cm) and terminal penetration distance ( $Z_\infty=0.7$  cm) could be chosen; these were used to calculate the solid line shown in Fig. 3 from Eq. (5). It is seen to agree quite well with the experimental points corresponding to a very wide range of sample materials and geometries.

The influence of the sample's thermal environment upon flux-jump kinetics has been investigated and will be reported elsewhere.<sup>9</sup>

The authors are grateful to Professor T. S. Hutchison and Dr. J. le G. Gilchrist for valuable comments and to R. A. Holman for assistance in the analysis of photographs.

\*Research supported by the Defence Research Board of Canada, Grant No. 9510-104.

<sup>1</sup>P. S. Swartz and C. P. Bean, *J. Appl. Phys.* **39**, 4991 (1968).

<sup>2</sup>S. L. Wipf, *Phys. Rev.* **161**, 404 (1967).

<sup>3</sup>K. Yamafuji, M. Takeo, J. Chikaba, N. Yano, and F. Irie, *J. Phys. Soc. Jap.* **26**, 315 (1969).

<sup>4</sup>B. B. Goodman and M. R. Wertheimer, *Phys. Lett.* **18**, 236 (1965).

<sup>5</sup>M. R. Wertheimer and J. le G. Gilchrist, *J. Phys. Rev. Chem. Solids* **28**, 2509 (1967),

<sup>6</sup>L. S. Wright, D. C. Baird, and M. R. Wertheimer in *Proceedings of the Twelfth International Conference on Low-Temperature Physics*, edited by Eizo Kauda (Academic of Japan, Kyoto, 1971), p. 465.

<sup>7</sup>Y. B. Kim, C. F. Hempstead, and A. R. Strnad, *Phys. Rev.* **139**, A1163 (1965).

<sup>8</sup>F. W. Grover, *Inductance Calculations* (Van Nostrand, Princeton, N.J., 1946), p. 35.

<sup>9</sup>R. B. Harrison, L. S. Wright, and M. R. Wertheimer (unpublished).

PHYSICAL REVIEW B

VOLUME 7, NUMBER 5

1 MARCH 1973

## Superconducting Energy Gaps from Magnetization Measurements: Pb-In System

C. T. Rao\* and L. W. Dubeck

*Physics Department, Temple University, Philadelphia, Pennsylvania 19122*

F. Rothwarf

*Electronics Technology and Devices Laboratory, Fort Monmouth, New Jersey 07703*

(Received 19 May 1972)

Isothermal-magnetization data have been obtained for a series of well-annealed chrome-plated Pb-In alloys of In composition between 30 and 80 at. % in the temperature range 1.90 °K to the appropriate transition temperature. The empirical relation proposed by Toxen involving the thermodynamic-critical-field data and the energy gap has been found to be valid over a wide range of values of the Ginzburg-Landau parameter  $\kappa$ , the electron mean free path  $l$ , and for both weak and strong coupling alloys. Consequently, it may be used to obtain the energy gap at  $T=0$  from the critical-field measurements both in the case of elemental and alloy superconductors. The experimentally determined Ginzburg-Landau parameters  $\kappa_1(T)$  and  $\kappa_2(T)$  show a stronger temperature dependence and are generally larger than predicted by existing weak coupling theories.

### I. INTRODUCTION

One of the characteristic features of superconductivity as described by the BCS theory is the existence of a gap  $\Delta(T)$  in the energy spectrum of single-particle Fermion excitations from the ground state. According to the BCS theory, for the weak coupling case the gap at  $T=0$  °K is  $2\Delta(0) = 3.52k_B T_c$ , where  $k_B$  is Boltzmann's constant and  $T_c$  is the transition temperature. In the so-called strong coupling superconductors  $2\Delta(0)$  assume values as large as  $4.6k_B T_c$ . Thus a measurement of  $2\Delta(0)$  for a superconductor provides an estimate of the strength of the electron-phonon interaction.

An interesting relationship between the critical field of a superconductor and its energy gap was pointed out by Toxen.<sup>1</sup> This empirical relation states that

$$\left. \frac{dh}{dt} \right|_{t=1} = \frac{\Delta(0)}{k_B T_c}, \quad (1)$$

where  $h = H_c(T)/H_c(0)$  is the reduced critical field, and  $t = T/T_c$  is the reduced temperature.  $H_c(T)$  and  $H_c(0)$  are the thermodynamic critical fields at temperatures  $T$  and 0 °K, respectively. Relation (1)

can be rewritten

$$\frac{T_c}{H_c(0)} \left. \frac{dH_c}{dT} \right|_{T=T_c} = \frac{\Delta(0)}{k_B T_c}. \quad (1')$$

Toxen,<sup>1</sup> using measured superconducting parameters, has shown that relation (1) is very well satisfied by both weak coupling and strong coupling elemental superconductors. It should be emphasized that  $|dh/dt|_{t=1}$  and  $\Delta(0)/k_B T_c$  depart from the values predicted by the BCS theory for weak coupling superconductors, but their ratio does not. Whereas BCS<sup>2</sup> predict  $|dh/dt|_{t=1} = 1.736$  and  $\Delta(0)/k_B T_c = 1.764$ , one finds for Pb<sup>3,4</sup>  $|dh/dt|_{t=1} = 2.13$  and  $\Delta(0)/k_B T_c = 2.17$ . Thus both these parameter increase as the coupling strength increases. There have been arguments<sup>5</sup> that relation (1) is just a numerical coincidence. Theoretically, Rothwarf<sup>6</sup> has shown that Toxen's proposed relation is consistent with the BCS theory if one uses the temperature dependence of the effective electron-electron interaction.

The BCS expression for the gap involves the effective electron-electron interaction  $V$  in the form

$$\Delta_k(T) = -\frac{1}{2} \sum_{k'} [V_{kk'}/E_{k'}(T)] \Delta_{k'}(T) \tanh \frac{1}{2} \beta E_{k'}(T), \quad (2)$$